

Frequency-dependent shear wave splitting beneath the Japan and Izu-Bonin subduction zones

Erin Wirth*, Maureen D. Long

Department of Geology and Geophysics, Yale University, New Haven, CT, United States

ARTICLE INFO

Article history:

Received 19 November 2009
Received in revised form 18 May 2010
Accepted 30 May 2010

Edited by: G. Helffrich

Keywords:

Shear wave splitting
Seismic anisotropy
Japan
Subduction dynamics
Mantle wedge

ABSTRACT

Despite its importance for our understanding of physical processes associated with subduction, the geometry of mantle flow in subduction zones remains poorly understood, particularly in the mantle wedge above subducting slabs. Constraints on mantle flow and deformation can be obtained by measurements of shear wave splitting, a valuable tool used to characterize the geometry and strength of seismic anisotropy. A complete characterization of shear wave splitting is particularly important for understanding the mantle wedge beneath Japan, which overlies multiple subduction zones with complex slab morphologies; previous studies indicate that the upper mantle beneath Japan exhibits complicated anisotropy that manifests itself in complex splitting patterns. To characterize better the geometry of mantle anisotropy beneath Japan, we analyzed direct S waves from local earthquakes originating in the subducting slabs for evidence of shear wave splitting using data from 54 broadband seismic stations in Japan's F-net array. In addition, both local S and teleseismic SKS phases were examined using data from four F-net stations in the Izu-Bonin arc. In order to characterize any frequency dependence of splitting parameters that may indicate the presence of complex anisotropy, we carried out our splitting analysis in two different frequency bands (0.02–0.125 Hz and 0.125–0.5 Hz). Our measurements indicate that shear wave splitting due to upper mantle anisotropy beneath Japan is highly complex and exhibits both dramatic spatial variations and a strong dependence on frequency.

© 2010 Elsevier B.V. All rights reserved.

1. Introduction

Elastic anisotropy is a nearly ubiquitous property of the upper mantle and manifests itself in the seismic wavefield in a variety of ways, including both body waves and surface waves. Shear wave splitting is a particularly valuable tool for characterizing seismic anisotropy because it is an unambiguous indicator of anisotropic structure and is generally unaffected by isotropic wavespeed heterogeneity (e.g., Silver, 1996; Savage, 1999; Long and Silver, 2009). Studies have shown that anisotropy in the upper mantle appears to be dominated by lattice preferred orientation (LPO) of mantle minerals, primarily olivine (e.g., Mainprice, 2007; Karato et al., 2008, and references therein), which results from deformation. Because of the causative link between dynamic processes in the upper mantle and the resulting anisotropy, the characterization of anisotropy using tools such as shear wave splitting can be used to gain valuable information about the geometry of mantle flow. The shear wave splitting parameters (fast polarization direction ϕ and delay time δt) give us information about the orientation of the olivine fast axis (related to the direction of mantle flow) and the strength

and extent of the anisotropy, respectively. Since shear wave splitting gives us information about anisotropy that can be related to strain-induced LPO, we can ultimately learn about mantle flow and deformation.

A complete characterization of upper mantle anisotropy is especially important in subduction zones. The presence of upper mantle anisotropy in subduction zones has been well documented (e.g., Ando et al., 1983; Fouch and Fischer, 1996; Fischer et al., 1998; Currie et al., 2004; Long and van der Hilst, 2005), but despite advances in our understanding of the structure of subducting slabs, the character of anisotropy and the pattern of mantle flow in subduction zones remain poorly understood. Previous studies of subduction zone anisotropy have yielded a wide variety of shear wave splitting patterns, including fast directions that are parallel, perpendicular, and (less often) oblique to the trench and a wide range of observed delay times. The classically accepted flow model for subduction zones, which is characterized by 2D corner flow in the mantle wedge and entrained flow beneath the slab, fails to account for the diverse observations. Consequently, other models have been proposed including trench-parallel flow in the mantle wedge (e.g., Smith et al., 2001), trench-parallel flow beneath the subducting slab (e.g., Russo and Silver, 1994), and 2D corner flow coupled with trench-parallel 3D return flow induced by trench migration (e.g., Long and Silver, 2008).

* Corresponding author. Tel.: +1 203 432 9808; fax: +1 203 432 3134.
E-mail address: erin.wirth@yale.edu (E. Wirth).

In addition to the variety of proposed flow models, differences in olivine LPO development in different parts of the subduction system have also been invoked to help explain the diversity of observed splitting patterns. Laboratory results have shown that in water-rich, high-stress environments such as those associated with subduction zones, the fast axes of olivine crystals will align perpendicular to the direction of mantle flow (Jung and Karato, 2001). The presence of this B-type olivine fabric in the shallow corner of the mantle wedge, in conjunction with trench-perpendicular flow, could explain the trench-parallel fast directions observed in subduction zone settings under the necessary physical conditions. It has also been suggested that the presence of partial melt (Holtzman et al., 2003) or a pressure-induced transition to B-type olivine fabric (Jung et al., 2009) might affect the relationship between mantle flow and the resulting anisotropy above or below the subducting slab, respectively.

A key difficulty in interpreting shear wave splitting measurements in subduction zones lies in isolating the effect of anisotropy in different parts of the subduction system (the overriding plate, the mantle wedge, the subducting slab, and the sub-slab mantle). Constraints on anisotropy in the mantle wedge and overriding plate can be obtained by measuring the splitting of local S phases; constraints thus obtained can then be used to isolate the effect of anisotropy in the slab and sub-slab mantle on teleseismic phases (e.g., Long and Silver, 2008). However, extreme care must be taken in this approach, since local S phases typically have shorter characteristic periods than teleseismic phases, and local S measurements are often made at higher frequencies than teleseismic splitting measurements (e.g., Nakajima and Hasegawa, 2004). Shear wave splitting measurements have been shown to be dependent on frequency in a variety of tectonic settings, including continental interiors (e.g., Clitheroe and van der Hilst, 1998; Fouch et al., 2004) and subduction zones (e.g., Marson-Pidgeon and Savage, 1997; Fouch and Fischer, 1998; Long and van der Hilst, 2006; Greve et al., 2008; Greve and Savage, 2009). From a finite-frequency point of view, waves with different periods will be sensitive to different volumes of mantle material (e.g., Alsina and Snieder, 1995; Favier and Chevrot, 2003; Long et al., 2008), so frequency-dependent shear wave splitting is likely an indication of heterogeneous anisotropy at depth.

2. Tectonic history and setting

In this study we focus on F-net stations located on the islands of Hokkaido, Honshu, Shikoku, and in the Izu-Bonin arc, regions affected by the subduction of the Pacific and Philippine Sea plates (Fig. 1). Here we briefly summarize the tectonic setting of our region of focus, largely based on an overview by Taira (2001). The formation of the Japanese island arc system is primarily the result of subduction of the Pacific plate, beginning sometime around the Permian. Currently, in northern Honshu and Hokkaido, the Pacific plate is subducting beneath the Kuril and Japan trenches and the Izu-Bonin trough to the south at a rate of ~ 10 cm/yr. This results in westward movement of Hokkaido and northeastern Honshu (relative to the Eurasian plate) at rates of 3–5 cm/yr. From south to north, the slab dip varies from $\sim 46^\circ$ in Izu, to $\sim 34^\circ$ in central Honshu, and to $\sim 29^\circ$ in northern Honshu (Syracuse and Abers, 2006). Continuing northward, the slab dip is $\sim 40^\circ$ in the Hokkaido corner and $\sim 50^\circ$ along the Kuril arc. Intermediate and deep earthquakes along the Pacific slab occur down to a depth of 670 km. Subduction of the Philippine Sea plate initiated more recently, around 15 Ma. This subduction resulted in an accretionary prism in the southwest Japan forearc. There is NW-directed subduction of the Philippine Sea plate beneath the Nankai trough at a rate of ~ 5 cm/yr, resulting in northwest movement of southwest Japan at 2–3 cm/yr.

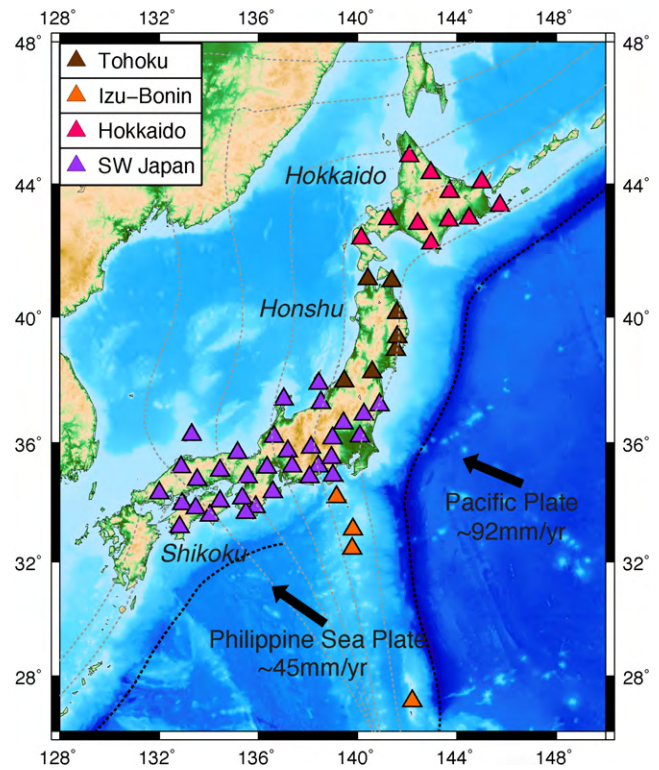


Fig. 1. Map showing topography and tectonic setting of Japan. Black dashed lines mark the trench locations with slab contours plotted every 100 km in gray (Gudmundsson and Sambridge, 1998). Colored triangles show the location of the 54 F-net stations examined in this study and are broken down by color into geographic region. Arrows indicate the direction of absolute plate motion for both the Pacific and Philippine Sea plates as given by the HS3-Nuvel1A model (Gripp and Gordon, 2002).

The Japanese arc system is characterized by an extensive distribution of active faults. In Hokkaido, the fault system is along the western side of the Hidaka Mountains, part of the thrust belt resulting from the Kuril forearc collision and backarc extension. The majority of these faults, as well as those located in northern Honshu, trend north-south, implying east-west directed compressional stress. Northern Honshu is characterized by active volcanic chains with high mountain ranges to the south due to interaction between the Okhotsk and Amur microplates. In southwest Honshu and part of Shikoku, faults run NW-SE and NE-SW; again indicating east-west compressional stress. The seismicity of Japan is directly related to the plate boundaries and active faults. Off the eastern coast of Hokkaido, the Kuril trench marks the location of plate boundary earthquakes. On land, the thrust belt to the west of the Hidaka Mountains is also seismically active. The Japan trench and Nankai trough off the coasts of northern Honshu and southwest Japan respectively, are known to generate frequent, high magnitude earthquakes. In addition, high magnitude events along the eastern margin of the Japan Sea can be attributed to the incipient subduction of the Amur microplate beneath northern Honshu and Hokkaido.

3. Shear wave splitting in Japan: previous results

In this study, we focus on shear wave splitting of local S phases originating in the subducting slabs beneath Japan and Izu-Bonin using data from the permanent broadband F-net array. Several previous studies have used shear wave splitting of direct S waves from local events to examine upper mantle anisotropy throughout Japan. In one such study, Salah et al. (2008) measured splitting from events

originating in the Pacific slab at a subset of F-net stations in central Japan. They observed fast directions parallel to the Nankai trench in the southernmost part of what we refer to as “southwest Japan” and parallel to the direction of plate motion at the northernmost part of the Izu-Bonin arc. Fouch and Fischer (1996) measured predominantly trench-parallel fast directions in the southernmost part of central Japan. Additionally, they measured fast directions parallel to the direction of downgoing plate motion in the Izu-Bonin arc. Delay times for the Salah et al. and Fouch and Fischer studies ranged from 0.1 to 1.25 s and 0.15 to 1.35 s using bandpass filters of 0.01–1 Hz and 0.1–1 Hz, respectively. In the northeastern Japan region of Tohoku, a general trend of trench-parallel fast directions close to the trench with a change in orientation to trench-perpendicular fast directions farther away from the trench, as well as an increase in delay time moving from east to west, has been well documented (Okada et al., 1995; Nakajima and Hasegawa, 2004; Nakajima et al., 2006). A comparison of our results with some of these previous studies can be found in Section 5. One of the major goals of this study is to examine shear wave splitting using uniform measurement procedures for the long-running broadband stations of the F-net array throughout Japan; while several previous studies have examined splitting in localized regions over a range of frequency bands, our aim is to provide a comprehensive, uniform database of local S splitting measurements that specifically addresses the frequency dependence of measured splitting parameters.

One of the most striking observations from previous studies of local S splitting in Japan is the observation by Nakajima and Hasegawa (2004) of a sharp transition in measured fast directions from trench-parallel in the forearc to trench-perpendicular in the backarc in the northern Honshu region; this transition has been interpreted as evidence for B-type olivine fabric in the mantle wedge (e.g., Nakajima and Hasegawa, 2004; Karato et al., 2008; Katayama, 2009). The delay times associated with these splitting measurements, however, were generally quite small (0.1–0.26 s in western Tohoku and 0.06–0.1 s in eastern Tohoku). These delay times are significantly smaller than those seen in other mantle wedges: larger delay times from direct S studies have been observed in several regions, including the Ryukyu arc (~0.75–1.25 s; Long and van der Hilst, 2006), Izu-Bonin (~0.6–1.7 s; Anglin and Fouch, 2005), the Marianas (~0.1–2.1 s; Pozgay et al., 2007), and Tonga (~0.5–1.7 s; Smith et al., 2001). However, because the Nakajima and Hasegawa (2004) study was carried out using high-frequency energy measured mainly at short-period stations (a bandpass filter with corner frequencies of 2 and 8 Hz was used), it is difficult to compare the results directly to those of other studies. In this study we reevaluate shear wave splitting beneath Tohoku in a frequency band that is more comparable to similar studies of local S splitting in order to facilitate comparisons among subduction zones globally.

In addition, shear wave splitting from teleseismic SKS phases recorded at F-net stations has previously been studied (Long and van der Hilst, 2005) and revealed that the anisotropic structure beneath Japan is highly heterogeneous, with many stations exhibiting complex teleseismic splitting patterns. A comparison of teleseismic splitting with local splitting measured over a range of frequencies at F-net stations in the Ryukyu arc (Long and van der Hilst, 2006) revealed that the source of anisotropy is mainly in the mantle wedge, and subsequent modeling studies (Long et al., 2007; Kneller et al., 2008) have shown that corner flow in the mantle wedge, with B-type olivine fabric dominating in the wedge corner, can explain the first-order aspects of the Ryukyu splitting patterns. In this paper, we present a local splitting dataset for F-net stations throughout Japan (excluding Ryukyu, but including four stations located in the Izu-Bonin arc) that is complementary to the teleseismic dataset of Long and van der Hilst (2005). By making shear wave splitting measurements over a wide range of frequencies, we

also bridge the large gap in frequency content between studies of teleseismic splitting in Japan (e.g., Fouch and Fischer, 1996; Long and van der Hilst, 2005) and previous studies of local splitting (e.g., Nakajima and Hasegawa, 2004; Nakajima et al., 2006; Salah et al., 2008, 2009), which have tended to rely on high-frequency energy.

4. Data and methods

The seismic data analyzed in this study were obtained from Japan's F-net network, an array of 83 STS-1 and STS-2 seismometers installed by the Japanese NIED (National Institute for Earth Science and Disaster Prevention) beginning in 1994. Data from F-net are made available by NIED on the Internet (www.fnet.bosai.go.jp). We processed data from fifty-four of these stations for events occurring between March 1995 and June 2008, depending on the dates of operation of individual seismometers.

We examined direct S phases from earthquakes originating in the subducting slabs for evidence of shear wave splitting, as well as teleseismic SKS phases recorded at four stations in the Izu-Bonin region (these stations were installed fairly recently and were not included in the teleseismic splitting study of Long and van der Hilst, 2005). In order to identify direct S phases suitable for analysis, we used seismic events with magnitudes ≥ 4.5 and depths greater than 80 km at epicentral distances between 0° and 6° . In addition, we restricted our analysis to waves arriving with an incidence angle less than $\sim 35^\circ$ to avoid the possibility of phase conversions at or near the free surface that may mimic splitting. This constraint resulted in a paucity of suitable S arrivals in central Honshu, perhaps due to the relatively shallow dip of the Pacific slab. For SKS phases, events with magnitudes ≥ 5.8 and at epicentral distances of 88–130° were used. Event locations for local and teleseismic earthquakes are shown in Fig. 2.

Shear wave splitting analysis was carried out using the SplitLab software package (Wüstefeld et al., 2007). Upon identification of the direct S or SKS phase arrival, a window encompassing at least one full period of the signal was manually chosen. A third order Butterworth filter was applied and the data were analyzed for evidence of shear wave splitting in each of the different frequency bands. To elucidate the effects of filtering on raw seismic data, the leftmost panels of Fig. 3 show an example seismogram in both its unfiltered and filtered form. Our “low” bandpass filter used corner frequencies of 0.02 and 0.125 Hz (periods between 8 and 50 s) and the “high” bandpass filter used corner frequencies of 0.125 and 0.50 Hz (periods between 2 and 8 s). This filtering convention matches that used by Long and van der Hilst (2006) in their study of local splitting in the Ryukyu arc; a key advantage of measuring local splitting at periods greater than ~ 8 s is that the overlap in frequency content with teleseismic phases makes a direct comparison more straightforward. Most events had significant energy in either the low band or high band, but not both.

Several steps were taken to guarantee the highest possible quality in the splitting dataset. First, for SKS phases both the rotation–correlation method and the transverse component minimization method of Silver and Chan (1991) were used. Several studies have demonstrated that the use of multiple measurement methods can ensure the reliability of the results (e.g., Levin et al., 2004; Vecsey et al., 2008; Long and Silver, 2009). Because the Silver and Chan method assumes that the shear arrival is radially polarized after conversion at the core–mantle boundary, the expected initial polarization direction corresponds with the station-to-event azimuth. Since direct S phases do not undergo this conversion, their initial polarization is unknown (unless predicted from a known focal mechanism or measured directly from the seismogram). Therefore, we relied mainly on the rotation–correlation method for measuring direct S splitting. The eigenvalue method

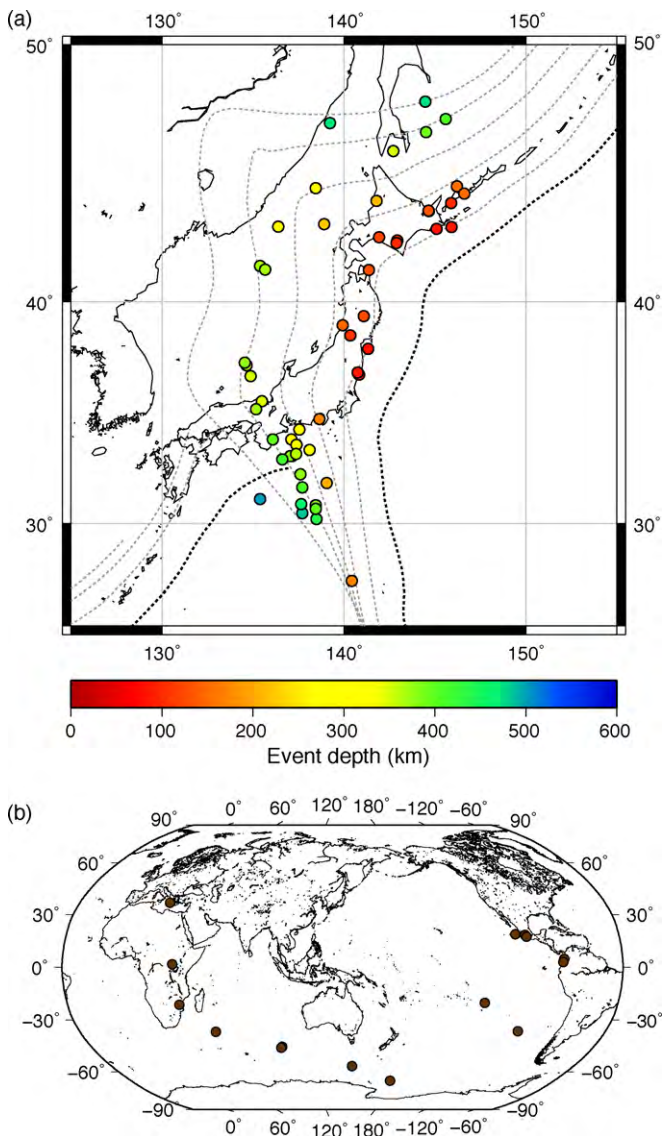


Fig. 2. (a) Map of local events used in direct S splitting analysis. Colors correspond to the event depth, as shown in the legend. (b) Map of teleseismic events used for SKS splitting.

proposed by Silver and Chan (1991), which aims to minimize the smallest eigenvalue of the corrected covariance matrix, was used as a secondary check on these measurements. We visually checked all initial and corrected particle motion diagrams, and the waveform quality of the horizontal components were checked by rotating the records into the “fast” and “slow” directions and visually inspecting the pulse shapes of the corrected seismograms.

In addition to using multiple methods to calculate the splitting parameters, measurements were also categorized using a ranking scheme. “Good” measurements had a high signal-to-noise ratio, clear waveform, displayed elliptical initial particle motion, and linear or nearly linear corrected particle motion (Fig. 3). For SKS phases, a ranking of “good” required agreement between the rotation–correlation and Silver and Chan methods, within $\pm 10^\circ$ for ϕ and ± 0.5 for δt . Measurements marked as “fair” either had agreement within $\pm 20^\circ$ for ϕ and ± 1.0 for δt , a lower quality waveform, or less linear corrected particle motion. A similar scheme was used for direct S phases with the rotation–correlation and eigenvalue methods. Finally, clear waveforms that displayed a high signal-to-noise ratio and linear or nearly linear initial particle motion were classified as null measurements. Null measurements result when

there is either no anisotropy present or when the incoming wave is already polarized in the fast or slow direction upon entering the anisotropic medium.

5. Results

5.1. Local S splitting results

For the direct S phases examined at 54 of the F-net stations, we obtained 38 high quality (classified as either “good” or “fair”) non-null splitting measurements in the low-frequency band, along with 60 null measurements. In the high-frequency band, 41 high quality non-null measurements were made along with 13 null measurements. For SKS phases examined at 4 stations in the Izu-Bonin region, we obtained 9 high quality splitting results and 8 null results. All of the low- and high-frequency non-null splitting results are shown in map view in Fig. 4a and b. Our measurements are plotted along with results from previous studies in Fig. 4c and d, and null measurements are shown in Fig. 5. A table of all individual splitting measurements can be found in the online supplementary material.

As we would expect due to the complexity of Japan’s tectonic setting, we see significant variation in fast direction results over small lateral distances. Moreover, there is considerably more scatter in the high-frequency band than in the low-frequency band (Fig. 6). However, there is enough consistency in the low-frequency band to identify several first-order features. In Hokkaido (Fig. 7), we see fast directions perpendicular to the trench and roughly parallel to the direction of plate motion; these measurements are mainly associated with deep (mostly greater than 350 km) earthquakes in the subducting Pacific slab. In Izu-Bonin, although the fast directions are fairly coherent and fall within a $\sim 30^\circ$ range, they can be interpreted as either subparallel to the direction of downgoing Pacific plate motion or parallel to the Japan trench (Fig. 8), as the subduction direction is highly oblique. The fast direction orientations in southwest Japan are significantly more complicated, likely because it overlies two adjacent subduction zones. This level of complexity is comparable to that observed in the teleseismic splitting patterns by Long and van der Hilst (2005) for this region. However, we can identify a group of fast directions that are close to perpendicular to the Japan trench, where the Pacific plate subducts beneath Eurasia, and another group of fast directions that tend to be parallel to the Nankai trench, where the Philippine Sea plate is subducting (Fig. 9). As previously mentioned, the fast directions obtained in the high-frequency band exhibit considerably more scatter. Even so, many of the results agree with the broad-scale patterns identified in the low-frequency measurements. No results were obtained for the Tohoku region in the low-frequency band, but in the high-frequency band we identify generally trench-parallel fast directions to the south with a gradual transition to trench-perpendicular moving northward (Fig. 10).

Perhaps the most striking result of this study is the drastic difference in measured delay times in our two different frequency bands. Delay times in the low-frequency band ranged from 0.85 s to 1.95 s with an average of 1.3 s. In the high-frequency band, δt ranged from 0.25 s to 1 s with an average of 0.6 s; this difference provides evidence for a strong dependence on frequency of mantle wedge shear wave splitting beneath Japan. It is also worthy to note the particularly low delay times in Tohoku, where results were only obtained in the high-frequency band. The delay times here ranged from 0.25 s to 0.35 s with an average of 0.3 s. The low δt is smaller than the detection limit at the periods included in the low-frequency band (~ 0.5 s of splitting for a characteristic period of ~ 10 s), which likely explains why no non-null measurements were identified in the low-frequency band.

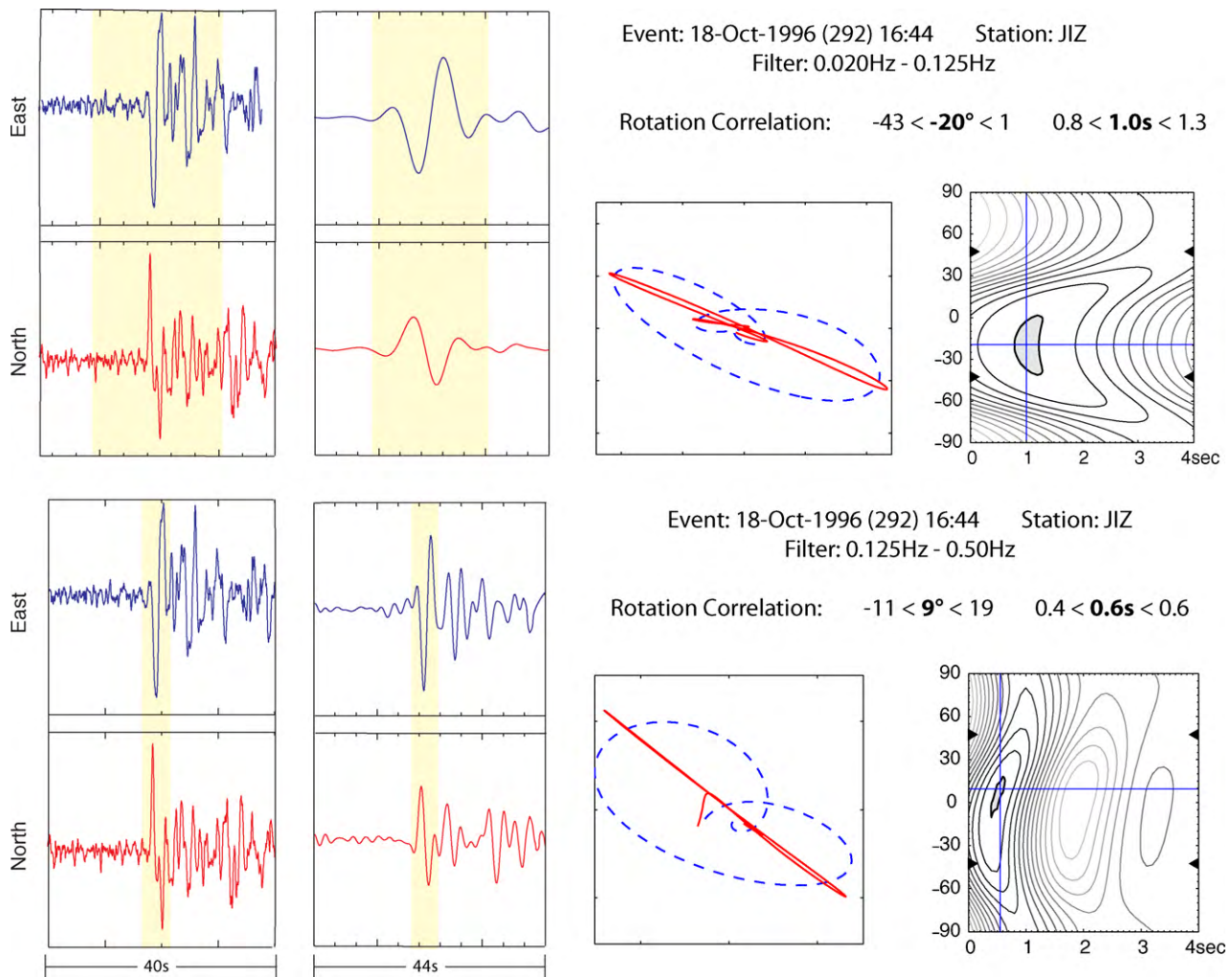


Fig. 3. Example of a low- and high-frequency direct S splitting measurement made for the same event-station pair using SplitLab (Wüstefeld et al., 2007). Fast direction and delay time along with corresponding uncertainties are given at the top. From left to right: unfiltered and uncorrected east and north components of motion; filtered and uncorrected components of motion, shaded region indicates the portion of the waveform used for splitting analysis; the uncorrected (dashed blue) and corrected (solid red) particle motion plots; plots of the 2σ error spaces. (For interpretation of the references to color in this figure legend, the reader is referred to the web version of the article.)

It is also relevant to examine the link between delay time and depth (Fig. 11). In this study, we find little, if any, relationship between delay time and depth of the event in either frequency band. This implies that to first order, the most significant source of anisotropy is likely in the shallow mantle wedge. However, because of the very complicated spatial patterns in the fast direction measurements, the comparison between delay times and event depths shown in Fig. 11 is not completely straightforward; in regions where there is a difference in fast direction between deep and shallow events (e.g., Hokkaido; Fig. 7), the data cannot be well explained with a single layer of anisotropy in the shallow wedge. Fig. 11 also demonstrates that there are few splitting measurements from earthquakes at depths between ~ 200 and 300 km in our dataset. This is due to the lack of seismicity at these depths and is consistent with the observation that globally, seismicity decreases nearly exponentially with depth up until 100 – 200 km, then begins to increase again until it reaches a well defined maximum (Isacks et al., 1968).

5.2. SKS splitting results

In order to complement the study of Long and van der Hilst (2005) which analyzed shear wave splitting for teleseismic events

using the F-net array, SKS data were examined for the four relatively new Izu-Bonin island stations (KZS, HJO, AOG, and OSW). The SKS results were significantly more complex than direct S results in the same region, displaying both plate-motion parallel and oblique fast directions (Fig. 8). However, the average delay time for SKS phases in the Izu-Bonin region was ~ 1.4 s, similar to the average delay time seen in direct S phases from deep slab earthquakes for the same area. The fast direction measurements made at station HJO which are subparallel to the direction of plate motion are confined to a backazimuth range of 160 – 260° . Meanwhile, the fast directions subparallel or oblique to the trench at both HJO and the other Izu-Bonin stations all lie outside this backazimuth range. While the backazimuthal coverage is insufficient to characterize the anisotropic structure beneath each station in detail, the complex splitting pattern observed at station HJO argues for complex structure, which likely takes the form of multiple layers of anisotropy beneath the station.

5.3. Null measurements

In addition to measurements of S phases that exhibited splitting, we also observed a large number of null measurements, particularly in the low-frequency band (Fig. 5). Such nulls can

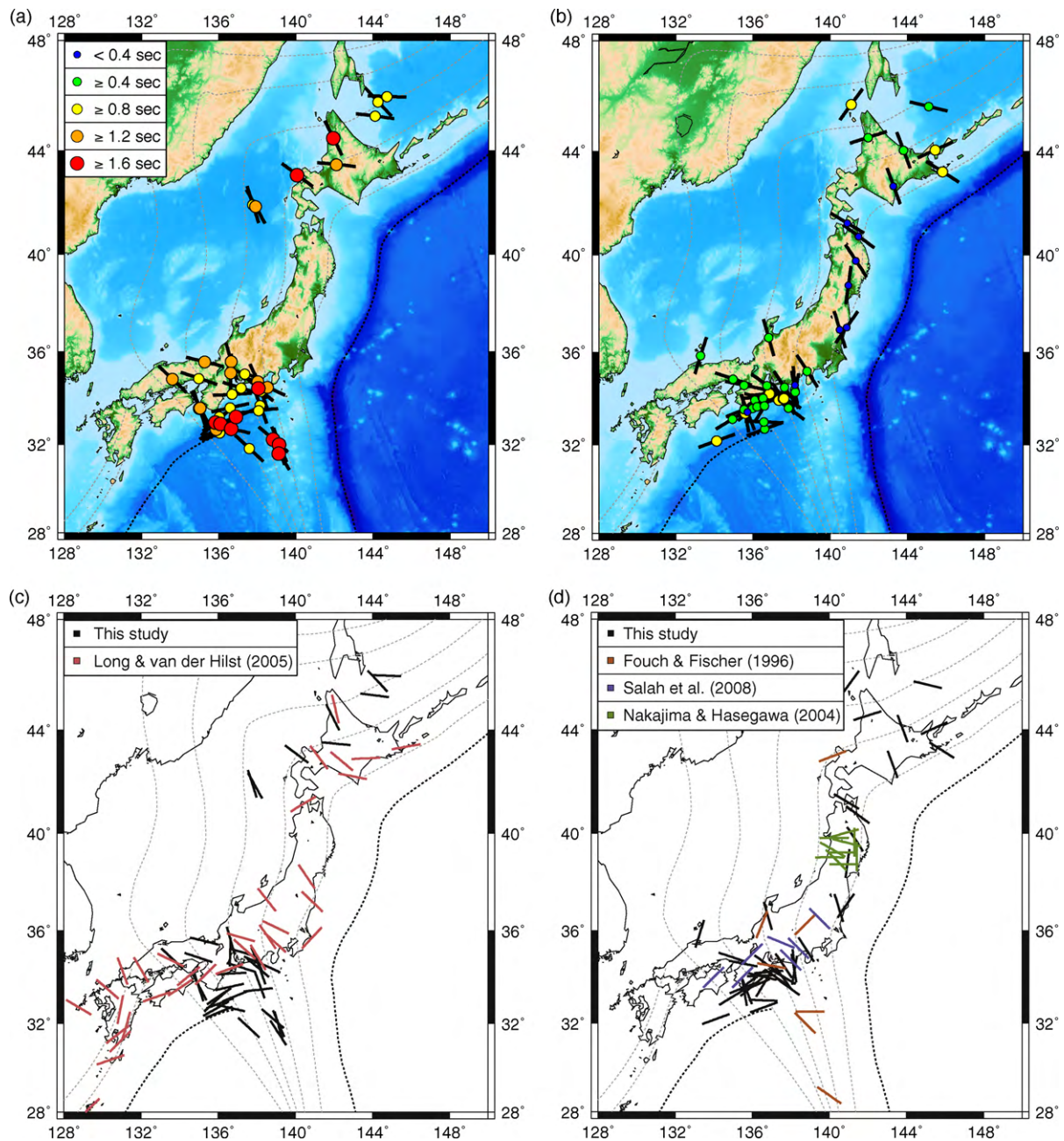


Fig. 4. Direct S splitting results for all high quality (good + fair) measurements made in the (a) low- and (b) high-frequency bands. Results are plotted at the midpoint between the event and station locations. Symbols are color-coded and scaled to reflect the magnitude of the delay time. Black bars are oriented parallel to the fast direction. (c) Our low-frequency and (d) high-frequency results (black bars) along with a rough sketch of fast direction orientations from previous shear wave splitting studies. For clarity, only select results that we deemed as representative for a particular region were plotted for each study. In (c), pink bars represent the SKS results of Long and van der Hilst at 0.02–0.125 Hz (2005). In (d), orange bars represent the local S results of Fouch and Fischer at 0.1–1 Hz (1996), purple bars represent the local S results of Salah et al. at 0.01–1 Hz (2008), and green bars represent the local S results of Nakajima and Hasegawa at 2–8 Hz (2004). (For interpretation of the references to color in this figure legend, the reader is referred to the web version of the article.)

be interpreted as potential fast or slow directions assuming that the wave came in with an initial polarization in the same direction as the fast or slow axis, resulting in no splitting. Of course, a null measurement could also be obtained if there were no anisotropy present along the raypath. In general, for local S phases we see null polarizations subparallel to the fast direction orientation predicted by non-null splitting measurements. Similarly, the majority of SKS null measurements replicate the complexity of the fast directions deduced from non-null measurements.

6. Discussion

6.1. The relationship between mantle flow and olivine fabric: mineral physics considerations

In order to correctly relate the orientation of the olivine fast axis to the direction of mantle flow, we must take mineral physics observations into account. The development of lattice preferred orientation of olivine is sensitive to variability in water content, stress, temperature, and (perhaps) pressure (e.g., Karato et al., 2008,

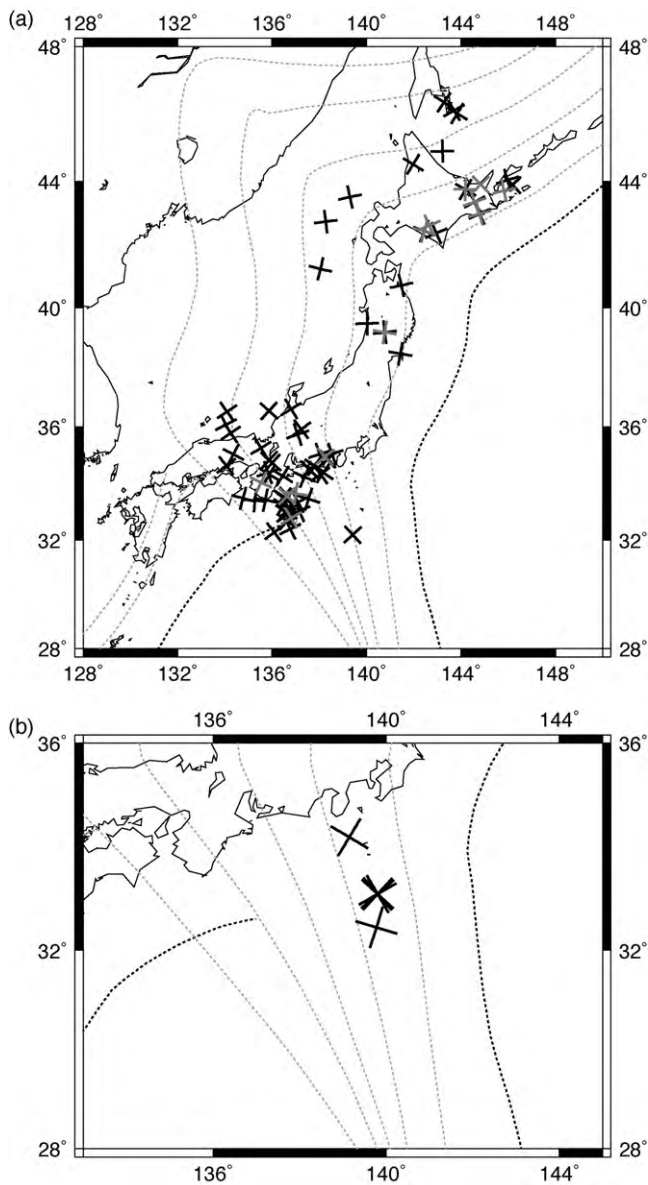


Fig. 5. (a) Map of all low (black) and high (gray) frequency “good” and “fair” null measurements for local events. Results are plotted as crosses at the midpoint between the station and event locations. Arms of the crosses are oriented in the direction of the measured initial polarization and the corresponding orthogonal direction. (b) Map of all high quality null measurements for SKS phases in the Izu-Bonin region using the low-frequency filter. Crosses are oriented as described in part (a) but plotted at the station location.

and references therein). Under lithospheric conditions of low water content and moderate temperature and stress, A-type olivine fabric is likely dominant. However in low stress, high water content conditions such as in the asthenosphere, the dominant fabric is probably either E- or C-type. In areas of high water content and above a critical stress threshold, we would expect the development of B-type fabric. In short, the transition from A- to E- to C-type olivine fabric is sensitive to changes in water content but not stress. The boundary between B- and C-type fabric is sensitive to changes in stress and temperature but not water content, where B-type fabric develops in the cooler, higher stress regions (Karato et al., 2008).

In subduction zones, we expect water content to play an important role in the development of LPO of olivine since dehydration of the subducting slab results in hydration of the overlying man-

tle wedge. We expect that the cool, high-stress environment in the shallow corner of the mantle wedge may provide the necessary conditions for B-type fabric development. This is important because unlike A-, C-, or E-type, the B-type fabric fast axis aligns perpendicular to the shear direction (Jung and Karato, 2001). Therefore, in areas where B-type fabric may be present, we cannot assume that the fast direction inferred from seismic observations aligns parallel to the direction of horizontal mantle flow.

Numerical modeling studies can help us better understand the necessary conditions for development of B-type olivine fabric in subduction zone settings. Kneller et al. (2005) modeled the effects of viscous coupling between the subducting slab and overlying mantle on the temperature and stress distribution within the mantle wedge. They found that partial viscous coupling, in which there is a velocity discontinuity along the slab–mantle wedge interface, limits the ability of the slab to entrain the overlying mantle. This decreases the extent to which hot material can penetrate into the shallow forearc mantle, creating conditions suitable for B-type olivine fabric. The core of the mantle wedge will still be a high temperature, low stress environment, more suitable for C- or E-type fabric. Increasing the depth of partial coupling increases the size of the region suitable for B-type fabric development.

The possibility of B-type olivine fabric in the shallow corner of the mantle wedge must be taken into account when interpreting shear wave splitting measurements in subduction zone settings. Assuming a simple 2D corner flow model and B-type olivine fabric in the cool corner of the mantle wedge, we would expect to see fast directions that align perpendicular to the flow direction, that is, subparallel to the trench. As we move farther away from the trench into the hotter core of the mantle wedge, we expect to see a transition from B-type fabric to C- or E-type. This will result in shear wave splitting fast directions that align perpendicular to the trench, parallel to the direction of mantle flow. Trench-parallel fast directions close to the trench are observed in several subduction zones including Ryukyu (Long and van der Hilst, 2006) where numerical modeling experiments have predicted that the conditions necessary for B-type fabric exist (Kneller et al., 2008). Observations of trench-parallel fast directions far into the backarc (e.g., Smith et al., 2001; Pozgay et al., 2007; Abt et al., 2009), where the conditions needed for B-type fabric are unlikely to exist, cannot be explained using a B-type fabric model.

6.2. Anisotropy and flow in the mantle wedge beneath Japan

For most of the stations examined in this study, we have restricted our analysis to direct S waves recorded from local earthquakes located in the subducting slab. The anisotropy responsible for this splitting signal must therefore reside in the mantle wedge, the overriding plate, or (perhaps) the very upper portion of the slab. Since contributions from the slab and overriding plate are likely to be much smaller than the average recorded delay time at low frequencies (~ 1.3 s) (e.g., Long and Silver, 2008), we infer that the primary contribution to the observed shear wave splitting is made by anisotropy in the mantle wedge above the subducting slabs. We further seek to interpret the measured fast directions in terms of flow patterns in the mantle wedge above the subducting Philippine Sea and Pacific plates. When analyzing the observed fast direction orientations, we chose to rely more heavily on the low-frequency results as the high-frequency data show considerably more scatter. In Hokkaido, Izu-Bonin, and the northernmost section of southwest Japan, we observe fast directions subparallel to the direction of Pacific plate motion. These measurements generally correspond to events that originate deep in the subducting slabs (>300 km); the associated raypaths mainly sample the deep part of the mantle wedge, as shown in Figs. 7c, 8b, and 9c. This appears to correspond well with a simple 2D corner flow model in the mantle wedge if

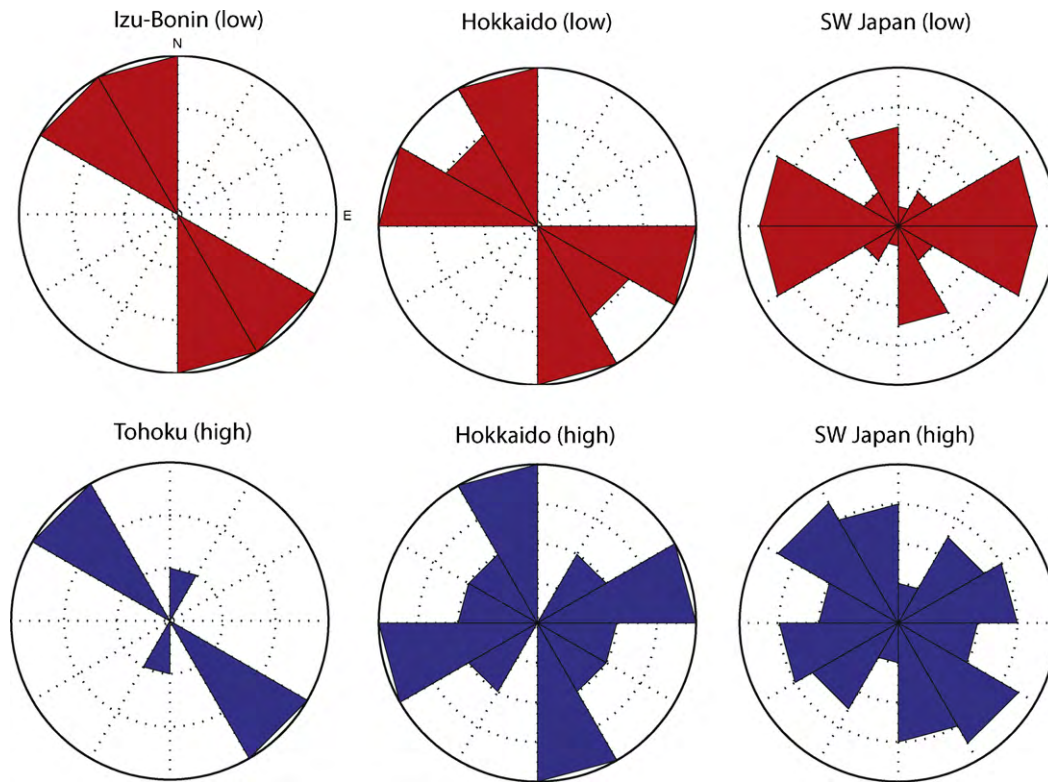


Fig. 6. Rose diagrams showing the measured fast directions in both frequency bands for direct S splitting results for different regions. Izu-Bonin high-frequency measurements and Tohoku low-frequency measurements are not shown due to the paucity of high quality results.

A-, C-, or E-type olivine fabric is assumed (e.g., Kneller et al., 2005). The generally convergence-parallel fast directions are roughly consistent with SKS results from Hokkaido and southwest Japan (Long and van der Hilst, 2005) as well as local S results from Izu-Bonin (Fouch and Fischer, 1996). However, it is noteworthy that while we do see some fast directions parallel to downgoing plate motion in Izu-Bonin, many of the fast directions could be considered closer to trench parallel. The average fast direction orientation is approximately N30°W, somewhat in between trench parallel (nearly N-S) and the direction of downgoing plate motion (~N60°W). Our results are similar to the N30°W fast direction orientation obtained by Anglin and Fouch (2005) in Izu-Bonin south of 30°N. However, they also documented highly complex splitting patterns north of 30°N (our primary region of study), measuring an average fast direction orientation of N31°E.

The interpretation of measured fast directions becomes significantly more complicated when we examine the region of southwest Japan (Fig. 9a). There are three identifiable dominant fast directions that appear in the data. There is a subset of measurements from events located deep in the Pacific slab recorded at stations located close to the Nankai trench that sample both the deep part of the Pacific mantle wedge and the shallow part of the Philippine Sea mantle wedge (Fig. 9c); these measurements are dominated by fast directions that are roughly parallel to the strike of the Nankai trench. Stations located farther away from the trench tend to exhibit fast directions that are trench-perpendicular or oblique. And as previously discussed, to the north we see a group of fast directions perpendicular to the Japan trench, in the direction of downgoing Pacific plate motion.

The variety of fast polarization directions measured in southwest Japan is inconsistent with the simplest possible 2D model for mantle wedge corner flow and likely reflects the complex slab morphology of the Pacific and Philippine Sea plates at depth. As previously stated, several models have been proposed to explain

the trench-parallel fast directions seen in many subduction zones, including trench-parallel flow in the mantle wedge (Smith et al., 2001), trench-parallel flow beneath the subducting slab (Russo and Silver, 1994), 2D corner flow coupled with trench-parallel 3D return flow induced by trench migration (Long and Silver, 2008), and the presence of B-type olivine fabric (Jung and Karato, 2001). In this case, trench-parallel flow beneath the slab can be eliminated as a cause because we are examining local S phases that do not sample the sub-slab mantle. Since our trench-parallel fast directions occur near the edge of the subducting Philippine Sea plate, it is possible that the observed results may be caused by 3D flow around the slab edge. We note, however, that Long and van der Hilst (2006) observed trench-parallel local S and SKS fast directions along the length of the Ryukyu arc (to the southwest of our region of interest) that extended up to 100 km away from the trench. They argued that this pattern was most likely due to the presence of B-type olivine fabric in the shallow part of the wedge, a hypothesis that was subsequently tested using 2D numerical models of wedge flow that predict the region of B-type fabric (Kneller et al., 2008). While we cannot rule out trench-parallel flow at the edge of the Philippine Sea slab, the trench-parallel fast directions observed in our study are consistent with the presence of B-type olivine fabric in the shallow wedge. The transition from trench-parallel fast directions close to the trench to trench-perpendicular fast directions farther from the trench that is predicted by the B-type olivine fabric model is also consistent with the observed pattern in southwest Japan.

6.3. Frequency-dependent versus path-dependent splitting

There were very few events that produced shear wave splitting measurements in both the low- and high-frequency bands. Therefore it is imperative to determine whether the differences between measurements made in different frequency bands are the result of a true frequency dependence of splitting parameters or an effect

of path dependence. If the distribution of raypaths between the high- and low-frequency datasets are dissimilar, then the observed differences could be attributed to sampling of different parts of the upper mantle volume rather than to a true dependence on frequency.

We found that local earthquakes beneath our study area rarely generated shear waves with significant energy in both of our frequency bands; therefore, we only made well-constrained splitting measurements for two event-station pairs. Event 1996.292 was recorded at station JIZ in SW Japan in both frequency ranges and is shown as an example in Fig. 3. In the low band, the fast direction orientation was -20° and the delay time was 1.0 s. In the high band, the fast direction was measured as 9° and the delay time was 0.6 s. Similarly, event 2000.112 was recorded at SW Japan station ISI and splitting was observed in both frequency bands. In the low band, fast direction orientation was -71° with a delay time of 1.0 s and in the high band fast direction was -71° with a 0.5 s delay time. While these two results show a strong dependence of delay time on frequency and a moderate dependence of fast direction orientation, it would be unwise to take two events as representative of the entire dataset. However, we note that there are many event-station pairs of measurements made in different frequency bands that traverse very similar paths. In Figs. 7c, 8b, 9c, and 10b, event-station pairs that produced splitting measurements in the low-frequency band have their paths colored in red, splitting measurements made in the high-frequency band have paths denoted in blue, and the two event-station pairs where splitting was observed in both bands have green paths. It is particularly clear in the region of SW Japan (Fig. 9c) that the collection of raypaths in both datasets are comparable and many individual pairs of low and high band measurements have very similar paths. Therefore, the most likely explanation for our observations is frequency-dependent shear wave splitting along comparable paths and not an effect of raypath distribution.

6.4. The implications of frequency-dependent splitting

A dependence of shear wave splitting parameters on frequency has been observed in a number of locations, including New Zealand (Marson-Pidgeon and Savage, 1997; Greve et al., 2008), the Marianas (Fouch and Fischer, 1998), and Australia (Clitheroe and van der Hilst, 1998). From a finite-frequency point of view, the size of the first Fresnel zone, the region over which sensitivity to anisotropic structure is greatest, increases with decreasing frequency (e.g., Alsina and Snieder, 1995; Favier and Chevrot, 2003). This implies that waves with different characteristic periods are sensitive to anisotropic structure over different scales; in particular, measurements made in lower frequency bands will tend to smooth out small-scale heterogeneities while high-frequency measurements are sensitive to these changes. Because the shear wave splitting sensitivity kernels depend on both frequency and heterogeneity in the background anisotropic structure (Long et al., 2008), in the presence of vertical or lateral heterogeneity shear wave splitting will be frequency dependent as well.

Our results reveal a strong dependence of splitting parameters upon frequency in Japan; we found average delay times of ~ 1.3 s at 0.02–0.125 Hz and ~ 0.6 s at 0.125–0.50 Hz, but only moderate dependence of fast direction orientation. This suggests that lateral and/or vertical changes in the strength of anisotropy are dominant over changes in geometry. Forward modeling studies in anisotropic media that vary with depth have suggested that high-frequency measurements tend to be biased towards upper layers of anisotropy (Saltzer et al., 2000), although subsequent work has shown that this bias towards shallow structure is not universal if three-dimensional heterogeneity is taken into account (Chevrot and Monteiller, 2009).

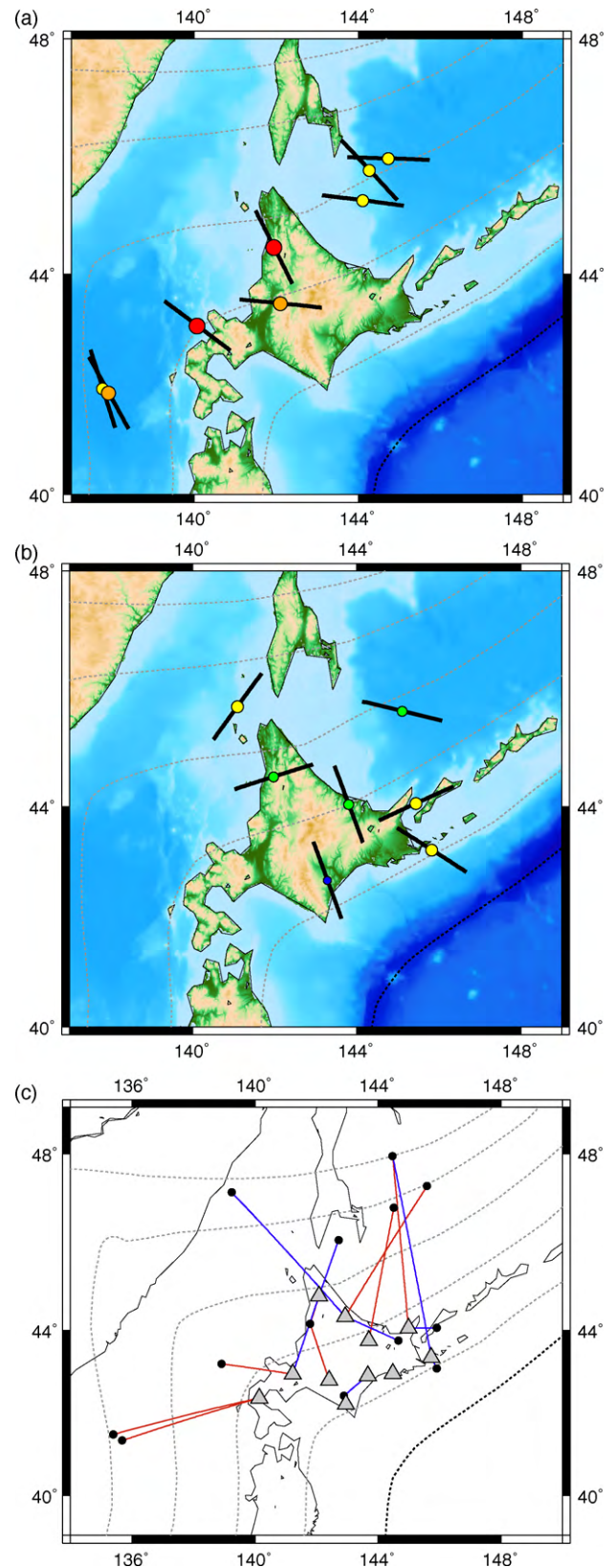


Fig. 7. Hokkaido splitting results in the (a) low-frequency band and (b) high-frequency band. (c) Map of station and event locations with corresponding raypaths for local events yielding splitting results in either frequency band. Red and blue raypaths represent splitting measurements made in the low- and high-frequency bands, respectively. (For interpretation of the references to color in this figure legend, the reader is referred to the web version of the article.)

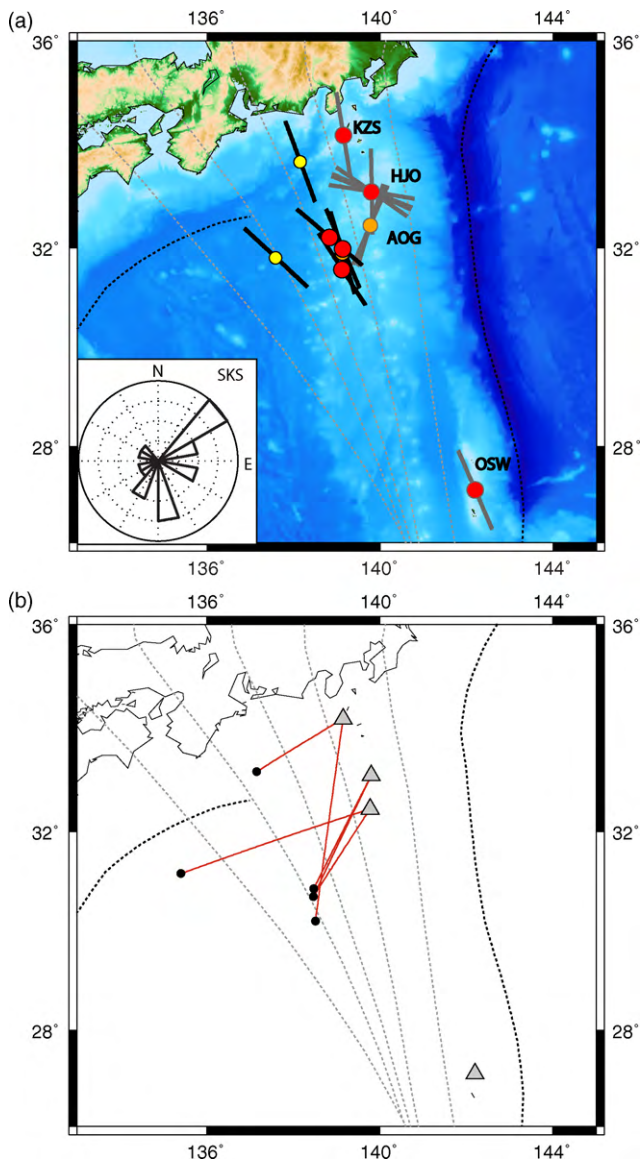


Fig. 8. (a) Izu-Bonin splitting results from local (black) and teleseismic (gray) events. Direct S measurements are plotted at the station-event midpoint while SKS measurements are plotted at the station location (labeled). Inset shows a circular histogram of backazimuthal coverage for null and non-null SKS measurements. (b) Map of station and event locations with corresponding raypaths for local events. The red raypaths indicate that splitting results were only obtained for measurements made in the low-frequency band. (For interpretation of the references to color in this figure legend, the reader is referred to the web version of the article.)

Since delay time measurements made in our high-frequency band are consistently lower than those made in the low-frequency band, it is likely that the strength of anisotropy is vertically heterogeneous beneath our study area.

We can also see the effects of frequency dependence upon delay time when comparing our results with previous studies. In particular, in eastern Tohoku we measured an average delay time of ~ 0.3 s at 0.125–0.50 Hz. Okada et al. (1995) recorded ~ 0.17 s delay times at 2–4 Hz, and Nakajima and Hasegawa (2004) obtained delay times of 0.06–0.1 s at 2–8 Hz. This variation in delay time with frequency is particularly relevant for studies that attempt to compare local S splitting with teleseismic splitting to isolate the contributions from anisotropy in different parts of the subduction system (e.g., Long and Silver, 2008). It is also germane for studies that have proposed different models to explain the pattern of shear wave splitting observed in northern Honshu (e.g., Tasaka et al., 2008;

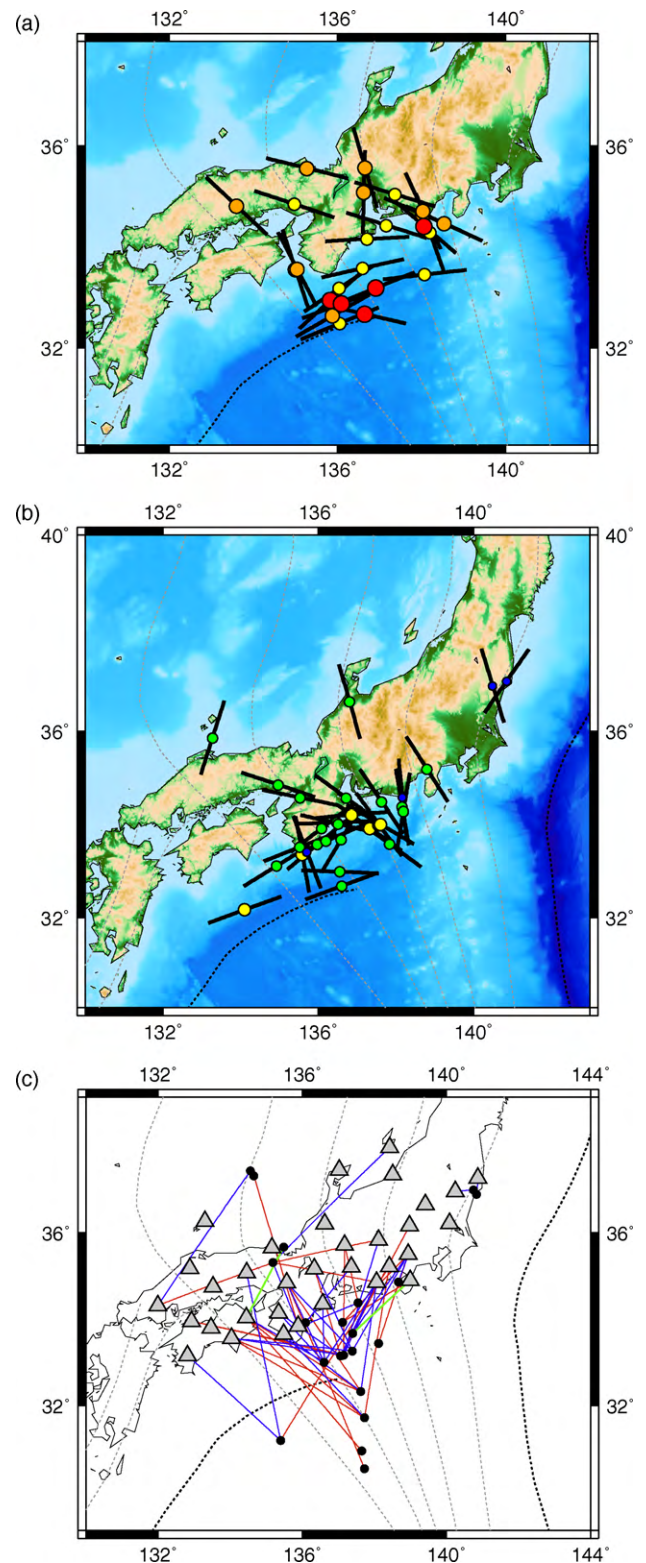


Fig. 9. Southwest Japan splitting results in the (a) low-frequency band and (b) high-frequency band. (c) Map of station and event locations with corresponding raypaths for local events yielding splitting results in either frequency band. Red and blue raypaths represent splitting measurements made in the low- and high-frequency bands, respectively. Green raypaths represent station-event pairs that yielded splitting results in both frequency bands. (For interpretation of the references to color in this figure legend, the reader is referred to the web version of the article.)

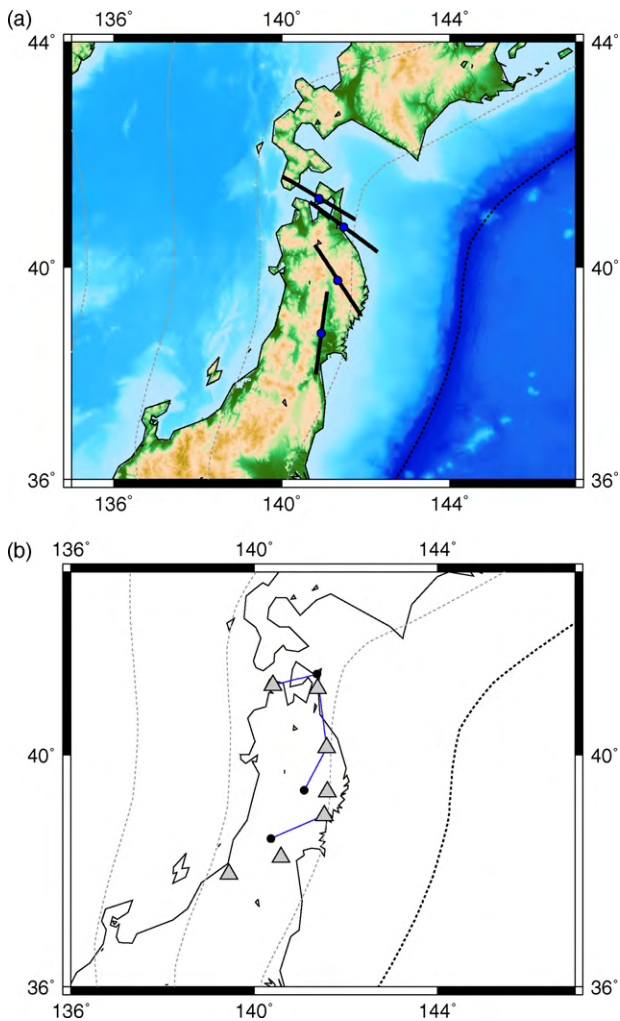


Fig. 10. (a) Tohoku splitting results in the high-frequency band. (b) Map of station and event locations with corresponding raypaths for local events. The blue raypaths indicate that splitting results were only obtained for measurements made in the high-frequency band. (For interpretation of the references to color in this figure legend, the reader is referred to the web version of the article.)

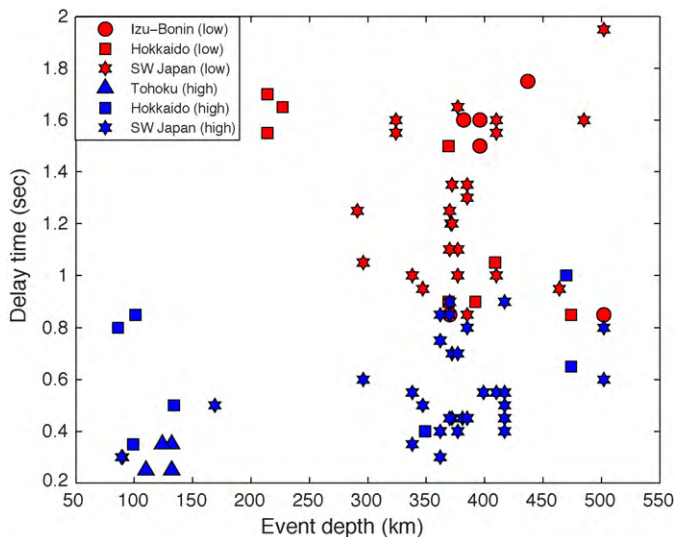


Fig. 11. Plot of measured delay time versus event depth for both low (red) and high (blue) frequency measurements. Different symbols are used to represent different regions as shown in the legend. (For interpretation of the references to color in this figure legend, the reader is referred to the web version of the article.)

Katayama, 2009), which explicitly try to match the observed delay times but do not generally take into account any dependence of δt on frequency.

Numerous mechanisms have been proposed to explain the frequency dependence of splitting parameters. These include porous flow through fractured rock (Liu et al., 2003), shape-preferred orientation of aligned melt bands (Greve et al., 2008), and small-scale heterogeneities (Marson-Pidgeon and Savage, 1997). We believe there are two scenarios that could potentially explain the strong dependence of delay times on frequency seen in our dataset. The first is that we are observing coupling between deformation in shallow and deeper layers (for example, the lower crust and lithospheric mantle, or the lithosphere and the asthenospheric mantle). If anisotropy in these layers resulted from similar deformation processes, we would expect to see a similar geometry of anisotropy in both layers and little scatter in fast direction orientation. We note, however, that we would expect a greater contribution to delay time from anisotropy in the upper mantle than from anisotropy in the crust, as crustal delay times in Japan have been shown to be on the order of 0.1 s (Kaneshima, 1990).

The other possibility is that the frequency dependence is a result of relatively shallow small-scale heterogeneities, likely in the crust or shallow mantle. If high-frequency measurements are indeed biased towards shallow structure (as suggested by Saltzer et al., 2000), this would explain the small delay times measured in our high-frequency band. However, as opposed to the previous explanation of coherency in deformation between shallow and deeper layers, we would expect anisotropy caused by small-scale heterogeneities in the crust to cause significant scatter in fast direction orientation between our two frequency bands. While some degree of difference in measured fast directions between our two datasets is observed, it is much less pronounced than the strong dependence of delay times on frequency, and it is unclear whether the scatter in fast direction orientation between the two frequency bands is significant. It is therefore difficult to distinguish between these two scenarios for producing frequency-dependent delay times. Despite this uncertainty, our results do demonstrate that the strength of relatively shallow and relatively deep anisotropy likely differs beneath Japan.

6.5. Explaining lateral variations in delay times in Japan

We obtained only a few high-quality splitting results for Tohoku (Fig. 10), and the limited spatial coverage of our dataset in this region makes it difficult to discriminate among different models for mantle flow. One robust observation from our work, however, is that the observed delay times in Tohoku are generally small (~ 0.3 s); this average delay time is significantly smaller than the regional average of ~ 0.6 s at high frequencies. It is also considerably smaller than the delay times observed in many mantle wedge settings in subduction zones worldwide (e.g., Long and Silver, 2008), where delay times of 1 s or more are fairly common. A key question, then, is how to explain this variability, and in particular how to explain the unusually small delay times observed in Tohoku compared to the much larger delay times we observe elsewhere in Japan. We are aware that some of the variability in measured delay times in our dataset may be due to differences in path length; for example, many of the measurements for Hokkaido come from deep events that have long path lengths in the deep part of the mantle wedge, while most of the measurements for Tohoku are from relatively shallow events. We do, however, observe a notable difference between the small delay times observed in Tohoku and other subduction zones with large delay times associated with relatively shallow events (e.g., Ryukyu; Long and van der Hilst, 2006).

One possibility is that there is a contribution from the shape-preferred orientation of partial melt pockets (e.g., Kendall, 1994) in

some parts of Japan, and that there is a regional variability in this contribution that is reflected in the measured delay times. Following the laboratory results of Zimmermann et al. (1999), Fischer et al. (2000) considered a model for wedge anisotropy in which melt filled cracks aligned at 20–30° from the maximum deviatoric compressive stress. They found that such an area of SPO melt could result in trench-parallel anisotropy. Because an active volcanic chain runs through central and northeastern Honshu, some amount of partial melt is almost certainly present in the mantle wedge. In the simplest case, we would expect this melt to be restricted to thin, vertical columns, confined to a small zone beneath the volcanoes (e.g., Gaetani and Grove, 2003), although it is likely that melt will be deflected some amount by solid-state flow in the wedge (e.g., Iwamori, 1998; Cagnioncle et al., 2007). A variable contribution to shear wave splitting from the SPO of melt could explain the variation in delay times in Japan if there was destructive interference between SPO-induced splitting and splitting due to the LPO of olivine; small delay times, in this scenario, would indicate that the presence of melt effectively cancels out the effect of anisotropy due to solid-state flow in the mantle wedge. It is unclear, however, if this mechanism could explain the observed variability; there are active volcanic chains in Hokkaido and Izu-Bonin as well, and presumably if the SPO of melt makes a significant contribution to splitting in Tohoku, it would do so in those regions as well. Additionally, one would expect the effect of melt SPO to be confined to a small region of the mantle directly beneath the volcanic chain, and the fact that small delay times are observed in Tohoku at stations that are not located in close proximity to the volcanic chain may be inconsistent with this scenario.

Another possibility is that the observed splitting in Tohoku mainly reflects anisotropy in the crust of the overriding plate, and not the mantle wedge, which would be consistent with the small delay times. There are few available measurements of crustal anisotropy in Japan, but observed delay times due to crustal anisotropy are generally on the order of ~0.1 s (Kaneshima, 1990). It is certainly possible, therefore, that the observed splitting at Tohoku stations is reflecting anisotropy in the crust (which is approximately 30–35 km thick; Taira, 2001) rather than the mantle wedge. This scenario, however, would require an explanation as to why the mantle wedge beneath Tohoku is apparently isotropic or nearly isotropic. Studies of other subduction zones have suggested an isotropic or only weakly anisotropic mantle wedge in South America (Polet et al., 2000), the Caribbean (Piñero-Feliciangeli and Kendall, 2008), and Java–Sumatra (Hammond et al., 2010). It has been proposed that for subduction systems where both trench migration and downdip motion of the slab are significant, there could be a contribution from both 2D corner flow and 3D flow induced by trench migration in the mantle wedge, and a spatially coherent flow field might not develop (Long and Silver, 2008). While this mechanism may explain an isotropic or nearly isotropic mantle wedge beneath Tokoku, it then becomes difficult to explain the relatively large delay times observed just to the north on Hokkaido. We do note, however, that our dataset for Hokkaido preferentially samples the deeper mantle wedge, while the Tohoku measurements primarily sample the shallow part of the wedge, so a direct comparison between the two may not be meaningful.

A third possibility for explaining the variability in mantle wedge delay times throughout Japan is to invoke differences in the degree of serpentinization of the mantle wedge. Serpentinization occurs in the forearc mantle of subduction zones due to dehydration processes of the subducting slab and the resulting hydration of the overlying mantle. A serpentinized mantle wedge has been proposed for Cascadia (Brocher et al., 2003; Bostock et al., 2002; Nikulin et al., 2009), central Japan (Kamiya and Kobayashi, 2000), and Izu-Bonin (Kamimura et al., 2002). Serpentinite is stable in cold regions of the forearc mantle and is associated with anomalously low seis-

mic velocities and a high Poisson's ratio (Christensen, 1996). In addition, the intrinsic anisotropy of some serpentinite phases is very large; single-crystal antigorite has an S wave anisotropy of ~38% (Kern, 1993), while the single-crystal shear anisotropy of olivine is ~18% (e.g., Isaak et al., 1989). In a detailed forward modeling study of wedge anisotropy in the Ryukyu subduction zone, just to the south of our study area, Kneller et al. (2008) found that while B-type olivine models could match the observed splitting, very strong B-type LPO would be required (up to ~14%). For this reason, they proposed that serpentinization of the forearc mantle might better explain the large shear wave splitting times seen in Ryukyu; subsequent experimental work on LPO in serpentinite has provided support for this hypothesis (Katayama et al., 2009). One potential explanation, then, for our relatively small delay times in Tohoku is that the degree of serpentinization of forearc mantle is small compared to elsewhere in Japan.

It is not surprising that we could potentially see serpentinite in the mantle wedge beneath southwest Japan considering the Philippine Sea plate is relatively young and hot, causing water to be released at shallow depths (Rüpke et al., 2004) and potentially causing widespread serpentinization of the forearc mantle. Beneath Tohoku, where the old, cold, Pacific slab is subducting, greater volumes of volatiles may be released deeper in the mantle wedge, and the forearc corner of the wedge may be dominated by olivine rather than serpentinite (Katayama et al., 2009). Then the fundamental question becomes how to explain the difference in splitting behavior between Tohoku and Hokkaido, which also overlie the subduction of the Pacific slab. One potential explanation for this is the difference in slab dip angle between the regions; along northeastern Honshu the slab is descending at an angle of ~30°, but the slab dip progressively steepens as we move northward. The slab dips at approximately 40° by the Hokkaido corner, and 50° along the Kuril arc (Syracuse and Abers, 2006). The relatively flat descent of the slab in northeastern Honshu might keep a greater volume of slab volatiles stable to a larger distance away from the trench, preventing widespread serpentinization of the forearc mantle. (Of course, the fact that there is arc volcanism above the Honshu slab suggests that there must be some volatile release at the arc.) A second potential explanation for the difference in observed delay times between Honshu and Hokkaido may be the difference in raypath geometry, as discussed above.

7. Summary

We have presented a dataset of 152 local and 17 SKS splitting measurements (null and non-null) from stations of the broadband F-net array located in Japan and Izu-Bonin in order to probe mantle anisotropy and flow in these subduction systems. It is clear from an examination of the splitting results presented here that anisotropy beneath Japan is highly complex and exhibits widespread heterogeneity. However, we can draw three important first order conclusions from this dataset. First, there is clear evidence for anisotropy in the mantle wedge near the islands of Hokkaido, Honshu, Izu-Bonin, and Shikoku. In southwest Japan, we observe fast directions oriented both trench-parallel close to the trench and trench-perpendicular farther away, which is consistent with the presence of B-type olivine fabric in the shallow corner of the mantle wedge. Second, we observe considerable lateral variations in delay time throughout Japan, with stations located in northern Honshu exhibiting relatively small delay times (~0.3 s) and stations elsewhere exhibiting delay times of ~0.6 s in the same frequency band. This difference may reflect lateral variations in melt SPO, in the degree of coherence of mantle wedge flow, or in the degree of serpentinization of the shallow mantle wedge. Third, the stations examined in this study exhibit a strong fre-

quency dependence of splitting parameters, which should be taken into account in any forward modeling studies that try to reproduce local S splitting patterns beneath the Japan and Izu-Bonin subduction zones as well as studies that seek to compare SKS and local S splitting measurements. This observation is consistent with other studies that have identified frequency-dependent splitting in subduction zone regions (e.g., Fouch and Fischer, 1998; Long and van der Hilst, 2006; Greve et al., 2008; Greve and Savage, 2009) and frequency-dependent splitting may well be a ubiquitous property associated with heterogeneous anisotropic structure in subduction zone mantle wedges. The dataset presented here is complementary to previous studies of teleseismic and local splitting in Japan and, in combination with the work of Long and van der Hilst (2005, 2006), provides a uniform splitting database for the stations of the permanent F-net array in the Japan, Ryukyu, and Izu-Bonin subduction zones. The comparison of the predictions from geodynamical models and mineral physics experiments with splitting observations in subduction zone settings is proving crucial in resolving their detailed anisotropic structure (e.g., Long et al., 2007; Kneller and van Keken, 2007; Kneller et al., 2008; Katayama, 2009), and recent theoretical work has provided a basis for taking into account finite-frequency effects in shear wave splitting studies (e.g., Favier and Chevrot, 2003; Long et al., 2008; Chevrot and Monteiller, 2009). Datasets such as the one presented here, which explicitly examine the dependence of shear wave splitting parameters on frequency, are likely to become more and more important in studies that seek to reconcile the predictions of geodynamical models with shear wave splitting observations, particularly in subduction zone settings.

Acknowledgements

We acknowledge the use of data from the F-net seismic network, which is operated and maintained by the Japanese National Research Institute for Earth Science and Disaster Prevention. This work was begun at the Department of Terrestrial Magnetism at the Carnegie Institution of Washington, where E.W. was supported through the Summer Intern Program in Geoscience, which is funded by NSF-EAR through the Research Experience for Undergraduates program. Additional support for this work was provided through NSF grant EAR-0911286. Some figures in this paper were generated using the Generic Mapping Tools (Wessel and Smith, 1991) and using the NGDC color palette for the ETOP01 global relief model. We thank Andreas Wüstefeld and his colleagues for making the SplitLab code freely available (<http://www.gm.univ-montp2.fr/splitting/>). Finally, we thank two anonymous reviewers for helpful suggestions that improved the manuscript.

Appendix A. Supplementary data

Supplementary data associated with this article can be found, in the online version, at doi:10.1016/j.pepi.2010.05.006.

References

- Abt, D.L., Fischer, K.M., Abers, G.A., Strauch, W., Protti, J.M., Gonzalez, V., 2009. Shear-wave anisotropy beneath Nicaragua and Costa Rica: implications for flow in the mantle wedge. *Geochem. Geophys. Geosyst.* 10, Q05S15, doi:10.1029/2009GC002375.
- Alsina, D., Snieder, R., 1995. Small-scale sublithospheric continental mantle deformation – constraints from SKS splitting observations. *Geophys. J. Int.* 123, 431–448.
- Ando, M., Ishikawa, Y., Yamazaki, F., 1983. Shear wave polarization anisotropy in the upper mantle beneath Honshu, Japan. *J. Geophys. Res.* 88, 5850–5864.
- Anglin, D.K., Fouch, M.J., 2005. Seismic anisotropy in the Izu-Bonin subduction system. *Geophys. Res. Lett.* 32, L09307, doi:10.1029/2005GL022714.
- Bostock, M.G., Hyndman, R.D., Rondenay, S., Peacock, S.M., 2002. An inverted continental Moho and serpentinization of the forearc mantle. *Nature* 417, 536–538.
- Brocher, T.M., Parsons, T., Trehu, A.M., Snelson, C.M., Fisher, M.A., 2003. Seismic evidence for widespread serpentinized forearc upper mantle along the Cascadia margin. *Geology* 31, 267–270.
- Cagnioncle, A.-M., Parmentier, E.M., Elkins-Tanton, L.T., 2007. Effect of solid flow above a subducting slab on water distribution and melting at convergent plate boundaries. *J. Geophys. Res.* 112, B09402, doi:10.1029/2007JB004934.
- Chevrot, S., Monteiller, V., 2009. Principles of vectorial tomography – the effects of model parameterization and regularization in tomographic imaging of seismic anisotropy. *Geophys. J. Int.* 179, 1726–1736.
- Christensen, N.I., 1996. Poisson's ratio and crustal seismology. *J. Geophys. Res.* 101, 139–156.
- Clitheroe, G., van der Hilst, R.D., 1998. Complex anisotropy in the Australian lithosphere from shear-wave splitting in broad-band SKS records. In: Brain, J., Dooley, J., Goleby, B., van der Hilst, R., Klootwijk, C. (Eds.), *Structure and Evolution of the Australian Continent*. Am. Geophys. Union Geodyn. Ser. vol. 26.
- Currie, C.A., Cassidy, J.F., Hyndman, R.D., Bostock, M.G., 2004. Shear wave anisotropy beneath the Cascadia subduction zone and western North American craton. *Geophys. J. Int.* 157, 341–353.
- Favier, N., Chevrot, S., 2003. Sensitivity kernels for shear wave splitting in transverse isotropic media. *Geophys. J. Int.* 153, 213–228.
- Fischer, K.M., Fouch, M.J., Wiens, D.A., Boettcher, M.S., 1998. Anisotropy and flow in Pacific subduction zone back-arcs. *Pure Appl. Geophys.* 151, 463–475.
- Fischer, K.M., Parmentier, E.M., Stine, A.R., Wolf, E.R., 2000. Modeling anisotropy and plate-driven flow in the Tonga subduction zone back arc. *J. Geophys. Res.* 105, 16181–16191.
- Fouch, M.J., Fischer, K.M., 1996. Mantle anisotropy beneath northwest Pacific subduction zones. *J. Geophys. Res.* 101, 15987–16002.
- Fouch, M.J., Fischer, K.M., 1998. Shear wave anisotropy in the Mariana subduction zone. *Geophys. Res. Lett.* 25, 1221–1224.
- Fouch, M.J., Silver, P.G., Bell, D.R., Lee, J.N., 2004. Small-scale variations in seismic anisotropy near Kimberley, South Africa. *Geophys. J. Int.* 157, 764–774.
- Gaetani, G.A., Grove, T.L., 2003. Experimental constraints on melt generation in the mantle wedge. In: Eiler, J.M. (Ed.), *Inside the Subduction Factory*. Am. Geophys. Union Geophys. Monogr. Ser. vol. 138, 107–134.
- Greve, S.M., Savage, M.K., 2009. Modelling seismic anisotropy variations across the Hikurangi subduction margin, New Zealand. *Earth Planet. Sci. Lett.* 285, 16–26.
- Greve, S.M., Savage, M.K., Hofmann, S.D., 2008. Strong variations in seismic anisotropy across the Hikurangi subduction zone, North Island, New Zealand. *Tectonophysics* 462, 7–21.
- Gripp, A.E., Gordon, R.G., 2002. Young tracks of hot spots and current plate velocities. *Geophys. J. Int.* 150, 321–361.
- Gudmundsson, O., Sambridge, M., 1998. A regionalized upper mantle (RUM) seismic model. *J. Geophys. Res.* 103, 7121–7136.
- Hammond, J.O.S., Wookey, J., Kaneshima, S., Inoue, H., Yamashina, T., Harjadi, P., 2010. Systematic variation in anisotropy beneath the mantle wedge in the Java–Sumatra subduction system from shear-wave splitting. *Phys. Earth Planet. Inter.* 178, 189–201.
- Holtzman, B.K., Kohlstedt, D.L., Zimmerman, M.E., Heidelbach, F., Hiraga, T., Hustoft, J., 2003. Melt segregation and strain partitioning: implications for seismic anisotropy and mantle flow. *Science* 301, 1227–1230.
- Isaak, D.G., Anderson, O.L., Goto, T., Suzuki, I., 1989. Elasticity of single-crystal forsterite measured to 1700 K. *J. Geophys. Res.* 94, 5895–5906.
- Isacks, B., Oliver, J., Sykes, L.R., 1968. Seismology and the new global tectonics. *J. Geophys. Res.* 73, 5855–5899.
- Iwamori, H., 1998. Transportation of H₂O and melting in subduction zones. *Earth Planet. Sci. Lett.* 160, 65–80.
- Jung, H., Karato, S.-i., 2001. Water-induced fabric transitions in olivine. *Science* 293, 1460–1463.
- Jung, H., Mo, W., Green, H.W., 2009. Upper mantle seismic anisotropy resulting from pressure-induced slip transition in olivine. *Nat. Geosci.* 2, 73–77.
- Kamimura, A., Kasahara, J., Shinohara, M., Hino, R., Shiobara, H., Fujie, G., Kanazawa, T., 2002. Crustal structure study at the Izu-Bonin subduction zone around 31 degrees N: implications of serpentinized materials along the subduction plate boundary. *Phys. Earth Planet. Inter.* 132, 105–129.
- Kamiya, S., Kobayashi, Y., 2000. Seismological evidence for the existence of serpentinized wedge mantle. *Geophys. Res. Lett.* 27, 819–822.
- Kaneshima, S., 1990. Origin of crustal anisotropy: shear wave splitting studies in Japan. *J. Geophys. Res.* 95, 11121–11133.
- Karato, S., Jung, H., Katayama, I., Skemer, P., 2008. Geodynamic significance of seismic anisotropy of the upper mantle: new insights from laboratory studies. *Annu. Rev. Earth Planet. Sci.* 36, 59–95.
- Katayama, I., 2009. Thin anisotropic layer in the mantle wedge beneath northeast Japan. *Geology* 37, 211–214.
- Katayama, I., Hirauchi, K., Michibayashi, K., Ando, J., 2009. Trench-parallel anisotropy produced by serpentine deformation in the hydrated mantle wedge. *Nature* 461, 1114–1117.
- Kendall, J.-M., 1994. Teleseismic arrivals at a mid-ocean ridge: effects of mantle melt and anisotropy. *Geophys. Res. Lett.* 21, 301–304.
- Kern, H., 1993. P- and S-wave anisotropy and shear-wave splitting at pressure and temperature in possible mantle rocks and their relation to the rock fabric. *Phys. Earth Planet. Inter.* 78, 245–256.
- Kneller, E.A., Long, M.D., van Keken, P.E., 2008. Olivine fabric transitions and shear wave anisotropy in the Ryukyu subduction system. *Earth Planet. Sci. Lett.* 268, 268–282.
- Kneller, E.A., van Keken, P.E., 2007. Trench-parallel flow and seismic anisotropy in the Marianas and Andean subduction systems. *Nature* 450, 1222–1225.

- Kneller, E.A., van Keken, P.E., Karato, S., Park, J., 2005. B-type olivine fabric in the mantle wedge: insights from high-resolution non-Newtonian subduction zone models. *Earth Planet. Sci. Lett.* 237, 781–797.
- Levin, V., Droznin, D., Park, J., Gordeev, E., 2004. Detailed mapping of seismic anisotropy with local shear waves in southeastern Kamchatka. *Geophys. J. Int.* 158, 1009–1023.
- Liu, E., Maultzsch, S., Chapman, M., Li, X.Y., Queen, J.H., Zhang, Z., 2003. Frequency-dependent seismic anisotropy and its implications for estimating fracture size in low porosity reservoirs. *Leading Edge* 22, 662–665.
- Long, M.D., de Hoop, M.V., van der Hilst, R.D., 2008. Wave-equation shear wave splitting tomography. *Geophys. J. Int.* 172, 311–330.
- Long, M.D., Hager, B.H., de Hoop, M.V., van der Hilst, R.D., 2007. Two-dimensional modeling of subduction zone anisotropy with application to southwestern Japan. *Geophys. J. Int.* 170, 839–856.
- Long, M.D., Silver, P.G., 2008. The subduction zone flow field from seismic anisotropy: a global view. *Science* 319, 315–318.
- Long, M.D., Silver, P.G., 2009. Shear wave splitting and mantle anisotropy: measurements, interpretations, and new directions. *Surv. Geophys.* 30, 407–461.
- Long, M.D., van der Hilst, R.D., 2005. Upper mantle anisotropy beneath Japan from shear wave splitting. *Phys. Earth Planet. Inter.* 151, 206–222.
- Long, M.D., van der Hilst, R.D., 2006. Shear wave splitting from local events beneath the Ryukyu arc: Trench-parallel anisotropy in the mantle wedge. *Phys. Earth Planet. Inter.* 155, 300–312.
- Mainprice, D., 2007. Seismic anisotropy of the deep Earth from a mineral and rock physics perspective. In: Schubert, G. (Ed.), *Treatise on Geophysics*, vol. 2, pp. 437–491.
- Marson-Pidgeon, K., Savage, M.K., 1997. Frequency dependent anisotropy in Wellington, New Zealand. *Geophys. Res. Lett.* 24, 3297–3300.
- Nakajima, J., Hasegawa, A., 2004. Shear-wave polarization anisotropy and subduction induced flow in the mantle wedge of northeastern Japan. *Earth Planet. Sci. Lett.* 225, 365–377.
- Nakajima, J., Shimizu, J., Hori, S., Hasegawa, A., 2006. Shear-wave splitting beneath the southwestern Kurile arc and northeastern Japan arc: a new insight into mantle return flow. *Geophys. Res. Lett.* 33, L05305, doi:10.1029/2005GL025053.
- Nikulin, A., Levin, V., Park, J., 2009. Receiver function study of the Cascadia megathrust: evidence for localized serpentinization. *Geochem. Geophys. Geosyst.* 10, Q07004, doi:10.1029/2009GC002376.
- Okada, T., Matsuzawa, T., Hasegawa, A., 1995. Shear-wave polarization anisotropy beneath the north-eastern part of Honshu, Japan. *Geophys. J. Int.* 123, 781–797.
- Piñero-Feliciangeli, L.T., Kendall, J.-M., 2008. Sub-slab mantle flow parallel to the Caribbean plate boundaries: inferences from SKS splitting. *Tectonophysics* 462, 22–34.
- Polet, J., Silver, P.G., Beck, S., Wallace, T., Zandt, G., Ruppert, S., Kind, R., Rudloff, A., 2000. Shear wave anisotropy beneath the Andes from the BANJO, SEDA, and PISCO experiments. *J. Geophys. Res.* 105, 6287–6304.
- Pozgay, S.H., Wiens, D.A., Conder, J.A., Shiobara, H., Sugioka, H., 2007. Complex mantle flow in the Mariana subduction system: evidence from shear wave splitting. *Geophys. J. Int.* 170, 371–386.
- Rüpke, L.H., Morgan, J.P., Hort, M., Connolly, J.A.D., 2004. Serpentine and the subduction zone water cycle. *Earth Planet. Sci. Lett.* 223, 17–34.
- Russo, R.M., Silver, P.G., 1994. Trench-parallel flow beneath the Nazca Plate from seismic anisotropy. *Science* 263, 1105–1111.
- Salah, M.K., Seno, T., Iidaka, T., 2008. Upper mantle anisotropy beneath central and southwest Japan: an insight into subduction-induced mantle flow. *J. Geodyn.* 46, 21–37.
- Salah, M.K., Seno, T., Iidaka, T., 2009. Seismic anisotropy in the wedge above the Philippine Sea slab beneath Kanto and southwest Japan derived from shear wave splitting. *J. Asian Earth Sci.* 34, 61–75.
- Saltzer, R.L., Gaherty, J., Jordan, T.H., 2000. How are vertical shear wave splitting measurements affected by variations in the orientation of azimuthal anisotropy with depth? *Geophys. J. Int.* 141, 374–390.
- Savage, M.K., 1999. Seismic anisotropy and mantle deformation: what have we learned from shear wave splitting? *Rev. Geophys.* 37, 65–106.
- Silver, P.G., 1996. Seismic anisotropy beneath the continents: probing the depths of geology. *Annu. Rev. Earth Planet. Sci.* 24, 385–432.
- Silver, P.G., Chan, W.W., 1991. Shear-wave splitting and subcontinental mantle deformation. *J. Geophys. Res.* 96, 16429–16454.
- Smith, G.P., Wiens, D.A., Fischer, K.M., Dorman, L.M., Webb, S.C., Hildebrand, J.A., 2001. A complex pattern of mantle flow in the Lau backarc. *Science* 292, 713–716.
- Syracuse, E.M., Abers, G.A., 2006. Global compilation of variations in slab depth beneath arc volcanoes and implications. *Geochem. Geophys. Geosyst.* 7, Q05017, doi:10.1029/2005GC001045.
- Taira, A., 2001. Tectonic evolution of the Japanese Island arc system. *Annu. Rev. Earth Planet. Sci.* 29, 109–134.
- Tasaka, M., Michibayashi, K., Mainprice, D., 2008. B-type olivine fabrics developed in the fore-arc side of the mantle wedge along a subducting slab. *Earth Planet. Sci. Lett.* 272, 747–757.
- Vecsey, L., Plomerova, J., Babuska, V., 2008. Shear-wave splitting measurements – problems and solutions. *Tectonophysics* 462, 178–196.
- Wessel, P., Smith, W.H.F., 1991. Free software helps map and display data. *EOS Trans. AGU* 72, 441.
- Wüstefeld, A., Bokelmann, G., Zaroli, C., Barruol, G., 2007. SplitLab: a shear-wave splitting environment in Matlab. *Comp. Geosci.* 34, 515–528.
- Zimmerman, M.E., Zhang, S., Kohlstedt, D.L., Karato, S.-i., 1999. Melt distribution in mantle rocks deformed in shear. *Geophys. Res. Lett.* 26, 1505–1508.